



1 **Reaction kinetics and multi-sulfur products formation of sulfur-**
2 **containing volatile organic compounds with OH radicals**

3 **Xun Rong¹, Lei Yao^{1,2,3*}, Chuang Li¹, Cong An¹, Gan Yang¹, Jiali Shen⁴, Runlong Cai^{1,2},**
4 **Douglas R. Worsnop^{4,5}, Lin Wang^{1,2,3,6,7}**

5 ¹ Shanghai Key Laboratory of Air Quality and Environmental Health, Department of Environmental
6 Science and Engineering, Jiangwan Campus, Fudan University, Shanghai 200438, China

7 ² Shanghai Institute of Pollution Control and Ecological Security, Shanghai 200092, China

8 ³ National Observations and Research Station for Wetland Ecosystems of the Yangtze Estuary, Shanghai
9 200438, China

10 ⁴ Institute for Atmospheric and Earth System Research/Physics, Faculty of Science, University of
11 Helsinki, 00014 Helsinki, Finland

12 ⁵ Aerodyne Research, Billerica, MA 01821, USA

13 ⁶ IRDR International Center of Excellence on Risk Interconnectivity and Governance on
14 Weather/Climate Extremes Impact and Public Health, Fudan University, Shanghai 200438, China

15 ⁷ Collaborative Innovation Center of Climate Change, Nanjing, 210023, China

16

17 *Correspondence: L. Y., email, lei_yao@fudan.edu.cn*

18

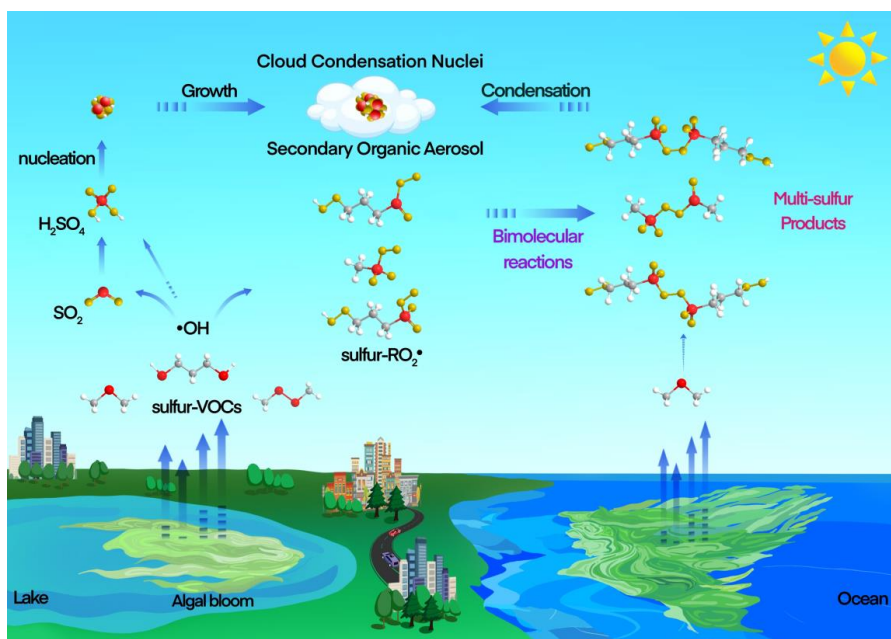
19 **Abstract.** Atmospheric sulfur-containing volatile organic compounds (sulfur-VOCs) have been
20 recognized as crucial precursors for gaseous sulfuric acid (H₂SO₄), particulate sulfate and secondary
21 organic aerosol (SOA) formation. However, their reaction kinetics and multi-sulfur product
22 formation remain poorly understood. This study presents a systematic kinetic investigation into
23 •OH-initiated oxidation of a series of sulfur-VOCs including thiols and sulfides, and the reaction
24 rates of dithiols and cyclic sulfides are generally higher than that of monothiols and acyclic sulfides.
25 It was further demonstrated that under low NO_x, sulfur-containing RO₂ radicals can undergo
26 bimolecular reactions forming low-volatility multi-sulfur products that enhance their SOA
27 formation potential. Additionally, many sulfur-VOCs investigated in our chamber experiments are
28 also identified from the emissions of algae samples collected from a major freshwater lake in China,
29 and similar multi-sulfur oxidation products were observed. These findings advance the kinetic and
30 mechanistic understanding of atmospheric sulfur-VOCs oxidation and suggest that the formation of
31 low-volatility multi-sulfur products and inorganic sulfur-containing species may contribute to SOA
32 production and new particle formation in marine and freshwater environments influenced by algal
33 emissions.

34

35 **Keywords:** sulfur-VOCs, reaction rates, multi-sulfur products, freshwater algae emissions,
36 secondary organic aerosol



37



38

39



40 **1 Introduction**

41 Atmospheric sulfur-containing volatile organic compounds (sulfur-VOCs) (e.g., dimethyl sulfide
42 (CH_3SCH_3 , DMS), methanethiol (CH_3SH), dimethyl disulfide ($\text{CH}_3\text{S}_2\text{CH}_3$, DMDS), and carbonyl
43 sulfide (OCS)) are important biogenic VOCs and mainly produced by degradation of sulfur-
44 containing amino acids and methylation of sulfides (Kietäväinen et al., 2025; Kilgour et al., 2021;
45 Li et al., 2022; Wang et al., 2023b). These compounds play a key role in the global atmospheric
46 sulfur cycle, and their atmospheric oxidation products such as sulfuric acid (H_2SO_4) and
47 methanesulfonic acid ($\text{CH}_3\text{SO}_3\text{H}$) are able to combine with basic species (e.g., NH_3 and amines) to
48 form new particles and particulate sulfate, which can contribute to the formation of cloud
49 condensation nuclei (CCN) and then have an effect on regional and global climate (Fiddes et al.,
50 2021; Jokinen et al., 2022; Revell et al., 2024; Wang et al., 2023a).

51 At present, it is widely recognized that marine ecosystems (e.g., phytoplankton) are the dominant
52 natural sources of atmospheric sulfur-VOCs, among which DMS is the dominant one and mainly
53 produced via the dimethylsulfoniopropionate (DMSP) metabolic pathway of phytoplankton (Novak
54 et al., 2022; Rocco et al., 2025). The importance of this source is further underscored by recent
55 satellite-based observations showing that, between 2003 and 2020, the global spatial extent of
56 coastal phytoplankton blooms expanded by 13.2% (+ 3.97 million km^2) and their frequency
57 increased by 59.2%, indicating an overall intensification of marine algae activity (Dai et al., 2023).
58 The measurements in marine boundary layer reported DMS mixing ratios ranging from tens to a
59 few hundred pptv with pronounced seasonal maxima in biologically productive waters (Zhao et al.,
60 2021). Co-emitted methanethiol is also detected and generally ranged from ~10 to 250 pptv (Mynard
61 et al., 2025; Novak et al., 2022; Rocco et al., 2025).

62 In addition to marine phytoplankton, freshwater algae are also recognized as important sources
63 of atmospheric sulfur-VOCs, including DMS, DMDS, and dimethyl trisulfide ($\text{CH}_3\text{S}_3\text{CH}_3$, DMTS),
64 which are released through amino acid degradation and methylation processes (Bao et al., 2024;
65 Huang et al., 2018; Li et al., 2022). This source is becoming particularly relevant in eutrophic
66 freshwater lakes experiencing frequent algal blooms. In China, around 85.4% of the 138 major
67 freshwater lakes with their areas larger than 10 km^2 suffer from varying degrees of eutrophication
68 (Wang et al., 2022). In such systems, concentrations of DMS, DMDS, and DMTS in the water
69 column commonly reach the microgram per liter level (Bao et al., 2024; Huang et al., 2018; Lu et
70 al., 2012; Yu et al., 2019a). Supporting the potential for atmospheric release, previous laboratory
71 and field studies have quantified sulfur-VOCs emission fluxes from freshwater lakes, showing that
72 DMS can be emitted at rates of several $\mu\text{mol m}^{-2} \text{d}^{-1}$, with emission intensity strongly modulated by
73 seasonality and trophic status of lakes (Li et al., 2022; Steinke et al., 2018). Many sulfur-VOCs have
74 been directly observed in the atmosphere near an inland freshwater lake (Dianshan Lake, Shanghai)



75 during winter-spring campaigns, with mixing ratios of DMS, methanethiol and DMDS can be up to
76 331.4 pptv, 183.8 pptv, and 153.6 pptv, respectively (Deng et al., 2025).

77 Once released into the atmosphere, sulfur-VOCs can rapidly react with hydroxyl radicals ($\bullet\text{OH}$).
78 The reaction rates between a few sulfur-VOCs (e.g., methanethiol, DMS, and DMDS (Abbatt et al.,
79 1992; Barnes et al., 1986; Cruz-Torres and Galano, 2007; Hashemi et al., 2019)) and $\bullet\text{OH}$ have been
80 well-established, with k_{OH} values of $\sim 3.3 \times 10^{-11} \text{ cm}^3 \text{ molecule}^{-1} \text{ s}^{-1}$ for methanethiol, $\sim 7.0 \times 10^{-12} \text{ cm}^3$
81 $\text{molecule}^{-1} \text{ s}^{-1}$ for DMS, and $\sim 2.3 \times 10^{-10} \text{ cm}^3 \text{ molecule}^{-1} \text{ s}^{-1}$ for DMDS, respectively (Atkinson et al.,
82 2004). These reactions play a critical role in determining the atmospheric lifetimes and
83 transformation pathways of these sulfur VOCs. There are significant differences in the reactivity of
84 sulfur-VOCs with different functional groups towards $\bullet\text{OH}$, with thiols and disulfides generally
85 exhibiting higher reactivity than that of mono-sulfides (Abbatt et al., 1992; Cruz-Torres and Galano,
86 2007; Hashemi et al., 2019; Tahan and Shiroudi, 2020). However, systematic understanding of
87 reaction kinetics of sulfur-VOCs with different functional groups towards $\bullet\text{OH}$ remains limited,
88 particularly for sulfur-VOCs with complex molecular structures which are increasingly detected in
89 field measurements. For instance, 1-propanethiol ($\text{CH}_3(\text{CH}_2)_2\text{SH}$), 2-propanethiol ($(\text{CH}_3)_2\text{CHSH}$),
90 methyl propyl disulfide ($\text{CH}_3\text{S}_2(\text{CH}_2)_2\text{CH}_3$), diethyl disulfide ($\text{CH}_3\text{CH}_2\text{S}_2\text{CH}_2\text{CH}_3$), and isopropyl
91 disulfide ($(\text{CH}_3)_2\text{CHS}_2\text{CH}(\text{CH}_3)_2$) have been detected from freshwater algae emissions, yet data on
92 their reaction kinetics with $\bullet\text{OH}$ remain scarce (Liu et al., 2021; Yu et al., 2019b; Zhou et al., 2024).
93 Therefore, it hinders accurate assessments of the chemical behavior and environmental impact of
94 these biogenic sulfur-VOCs in the atmosphere, particularly in aquatic environments (e.g., huge
95 freshwater lakes) where algae blooms frequently occur.

96 Previous studies on the reaction mechanisms between some sulfur-VOCs and $\bullet\text{OH}$ have
97 established a relatively comprehensive framework (Berndt et al., 2024; Goss and Kroll, 2023; Shen
98 et al., 2022; Ye et al., 2022). The initial steps typically involve the formation of sulfur-containing
99 radicals (sulfur- $\text{R}\bullet$) via H-extraction or $\bullet\text{OH}$ -addition, which then combine with O_2 to generate
100 various sulfur-containing RO_2 radicals (sulfur- $\text{RO}_2\bullet$) (Berndt et al., 2023; Goss and Kroll, 2023;
101 Shen et al., 2022). Among these, sulfides primarily form α -carbon peroxy radicals (e.g.,
102 $\text{CH}_3\text{SCH}_2\text{OO}\bullet$), while thiols and disulfides tend to generate sulfur-centered peroxy radicals (e.g.,
103 $\text{RSOO}\bullet$) (Berndt et al., 2023; Goss and Kroll, 2023; Lily et al., 2023). Although the unimolecular
104 reactions (e.g., H-migration) and bimolecular reaction pathways involving NO_x and $\text{HO}_2\bullet$ of these
105 sulfur- $\text{RO}_2\bullet$ species have been investigated, the bimolecular reactions between sulfur- $\text{RO}_2\bullet$ and
106 sulfur- $\text{R}'\text{O}_2\bullet$ remain poorly characterized (Berndt et al., 2023; Jernigan et al., 2022; Shen et al.,
107 2022).

108 This study systematically investigated the reaction kinetics and multi-sulfur products formation
109 of 11 sulfur-VOCs with $\bullet\text{OH}$ using a Teflon chamber together with a Vocus proton transfer reaction



110 long-time-of-flight mass spectrometry (Vocus-PTR-LToF-MS, ToFwerk AG) and a nitrate-based
111 chemical ionization long-time-of-flight mass spectrometry (nitrate-CI-LToF-MS, Aerodyne
112 Research). To investigate the relationship between the reaction rates and their molecular structures,
113 these 11 sulfur-VOCs were divided into 5 classes, which are monothiols (i.e., ethanethiol (C_2H_6S),
114 1-propanethiol (C_3H_8S), and 2-propanethiol (C_3H_8S)), dithiols (i.e., 1,2-ethanedithiol ($C_2H_6S_2$), and
115 1,3-propanedithiol ($C_3H_8S_2$)), acyclic sulfides (i.e., dimethyl sulfide (C_2H_6S), methyl ethyl sulfide
116 (C_3H_8S), and bis(methylthio)methane ($C_3H_8S_2$)), cyclic sulfides (i.e., trimethylene sulfide (C_3H_6S),
117 and 1,3-dithiolane ($C_3H_6S_2$)) and disulfides (dimethyl disulfide ($C_2H_6S_2$)) (Table 1). Moreover, the
118 emitted VOCs from freshwater algae samples taken from a huge freshwater lake (i.e., Taihu lake,
119 China) and their oxidation products by $\bullet OH$ were also investigated. Similar sulfur-VOCs and multi-
120 sulfur products were also observed from VOCs emitted from freshwater algae samples and their
121 oxidation products, which demonstrates the atmospheric relevance of our selected sulfur-VOCs and
122 their atmospheric transformation mechanisms in our study.

123 **2 Materials and methods**

124 **2.1 Chamber experiments of 11 sulfur-VOCs with $\bullet OH$**

125 The selected 11 high-purity ($\geq 96\%$) sulfur-VOCs liquid standards (Sigma-Aldrich and Macklin)
126 were listed in Table S1. These liquid standards were then used to generate individual sulfur-VOC
127 standard gases with our laboratory partial-pressure gas mixing system (Li et al., 2025; Wang et al.,
128 2020). The experimental setup is shown in Figure S1. A 0.53 m^3 polytetrafluoroethylene (FEP)
129 chamber was employed to conduct atmospheric oxidation experiments of sulfur-VOCs with $\bullet OH$.
130 The experimental conditions including the initial mixing ratios of sulfur-VOCs, O_3 concentration,
131 and relative humidity (RH), are summarized in Table 1. The OH radicals were generated by
132 photolysis of O_3 under humid condition using a 253 nm ultraviolet lamp (Philips TUV 16W).

133 During these experiments, the evolution of 11 sulfur-VOCs was monitored by a Vocus-PTR-
134 LToF-MS, and their oxidation intermediates and products (e.g., sulfur-containing peroxy radicals,
135 gaseous H_2SO_4 and multi-sulfur products) were detected using a nitrate-CI-LToF-MS. The
136 estimation of wall and dilution loss of sulfur-VOCs in our chamber was described in Text S3. The
137 procedure used to quantify sulfur-containing oxygenated organic molecules (sulfur-OOMs) was
138 described in Text S5. In addition, an ozone monitor (Thermo, 49i) and a temperature and humidity
139 sensor (Vaisala HMP110) were used to record O_3 concentration and monitor environmental
140 conditions in the chamber. Due to the chamber is not collapsible, a make-up flow of 15 L/min high-
141 purity zero air generated from zero air generator (AADCO 737 series) was continuously introduced
142 to the chamber and a RH of 20–25% was maintained.

Table 1. Experimental conditions of 11 sulfur-VOCs with •OH under temperature 291±1 K and 1 atm.

Exp.	Species	sulfur-VOCs	Formulae	Molecular structure	Precursor conc. (ppbv)	[O ₃] (ppbv)	Relative humidity (%)
1	Monothiols	ethanethiol	C ₂ H ₆ S		0.90	33.5	25.1
2					1.50	31.7	24.3
3		1-propanethiol	C ₃ H ₈ S		45.39	32.4	17.4
4		2-propanethiol	C ₃ H ₈ S		1.10	31.8	24.0
5	Dithiols	1,2-ethanedithiol	C ₂ H ₆ S ₂		1.77	31.5	24.0
6					0.65	30.0	23.9
7					1.67	30.5	24.3
8		1,3-propanedithiol	C ₃ H ₈ S ₂		2.84	30.0	22.8
9					2.33	31.1	24.0
10	Acyclic sulfides	dimethyl sulfide	C ₂ H ₆ S		0.83	30.9	24.0
11					0.94	31.7	22.0
12		methyl ethyl sulfide	C ₃ H ₈ S		0.28	29.5	24.2
13					0.29	31.7	24.3
14	Cyclic sulfides	bis(methylthio)methane	C ₃ H ₈ S ₂		10.61	30.4	20.9
15		trimethylene sulfide	C ₃ H ₆ S		0.79	28.6	24.3
16				0.62	29.7	25.3	
17		1,3-dithiolane	C ₃ H ₆ S ₂		1.40	35.0	22.8
18					1.23	31.7	24.3
19	Disulfides	dimethyl disulfide	C ₂ H ₆ S ₂		0.74	33.0	25.5
20					0.75	29.0	24.7





145 **2.2 Characteristic of VOC emission from freshwater algae**

146 Fresh water samples with algae were collected from Taihu Lake (~2338.1 km²), China, which is
147 the third largest freshwater lake in China (Qin et al., 2019; Wang et al., 2023c), at the Taihu Lake
148 Ecosystem Research Station (Figure S2 a). In the past years, frequent large-scale algal blooms often
149 occurred in Taihu Lake due to anthropogenic nutrient inputs and endogenous pollutant releases in
150 summer (Wang et al., 2019; Xu et al., 2021). Therefore, the water samples with algae taken from
151 Taihu Lake were treated as representative samples of freshwater algae.

152 During the emission characterization process, water samples were divided into 12 petri dishes
153 (with a total exposed liquid surface area of 0.213 m²) and placed in the chamber for 18 hours at the
154 temperature of ~21°C to allow the release of VOCs (Figure S2 b). After that, ~90 ppb of O₃ was
155 injected into the chamber and two 253 nm UV lamps were turned on to generate •OH by photolysis
156 of O₃ under humid conditions (Figure S3). A Vocus-PTR-LToF-MS, which was calibrated using
157 selected sulfur-VOC standards (Text S4), was employed to measure and identify sulfur-VOCs and
158 other VOC species released from freshwater algae, as well as their low-oxygenated oxidation
159 products, while a nitrate-CI-LToF-MS was used to identify the mono-sulfur and multi-sulfur
160 products derived from the reactions of sulfur-VOCs from algal source with •OH.

161 **3 Results and discussion**

162 **3.1 Rate constants of sulfur-VOCs with •OH**

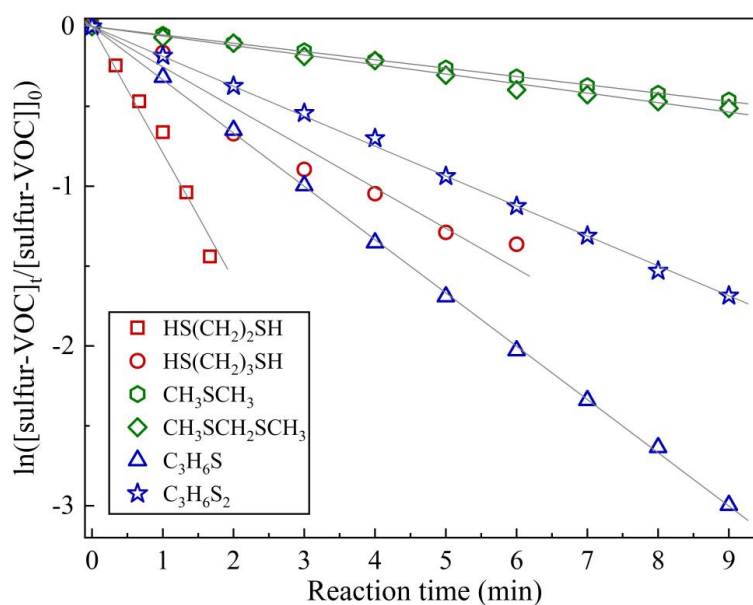
163 The reaction rates were derived based on Eq. (1) in Text S2. By monitoring the change in
164 concentrations of sulfur-VOCs over time, a linear relationship was established. To estimate the •OH
165 concentration in the chamber, DMS was employed as a reference compound, based on its well-
166 established temperature-dependent reaction rate with •OH (Text S2). The estimated •OH
167 concentration was $4.42 \pm 0.08 \times 10^7$ molecules cm⁻³. Using the estimated •OH concentration, the
168 reaction rate constants of 10 other sulfur-VOCs with •OH were subsequently determined (Table 2).

169 The order of magnitude of reaction rates ranged from 10⁻¹¹ to 10⁻¹⁰ cm³ molecule⁻¹ s⁻¹ (Table 2),
170 with pronounced differences among different classes of sulfur-VOCs, including thiols, dithiols,
171 acyclic sulfides, cyclic sulfides, and disulfide. Besides the reference compound DMS which was
172 used to estimate •OH concentration in the chamber, Figure 1 presents the linear fitting results for 5
173 sulfur-VOCs, whose reaction rates remain scarce in previous studies. These 5 sulfur-VOCs and their
174 reaction rates are 1,2-ethanedithiol ($2.99 \pm 0.10 \times 10^{-10}$ cm³ molecule⁻¹ s⁻¹), 1,3-propanedithiol (8.46
175 $\pm 0.53 \times 10^{-11}$ cm³ molecule⁻¹ s⁻¹), bis(methylthio)methane ($1.49 \pm 0.11 \times 10^{-11}$ cm³ molecule⁻¹ s⁻¹),
176 trimethylene sulfide ($1.15 \pm 0.02 \times 10^{-10}$ cm³ molecule⁻¹ s⁻¹), and 1,3-dithiolane ($6.11 \pm 0.13 \times 10^{-11}$
177 cm³ molecule⁻¹ s⁻¹), respectively (Table 2).

178 The corresponding fittings for the remaining 5 sulfur-VOCs, which have been studied previously,



179 are also provided in Figure S4. The obtained reaction rates of these 4 sulfur-VOCs (i.e., ethanethiol,
180 1-propanethiol, 2-propanethiol and methyl ethyl sulfide) from our experiments are consistent with
181 that reported by previous studies, ensuring our experimental results (Table 2) (Barnes et al., 1986;
182 Wang et al., 2011; Wine et al., 1984). However, a notable discrepancy was observed for DMDS,
183 with the current value ($1.03 \pm 0.02 \times 10^{-10} \text{ cm}^3 \text{ molecule}^{-1} \text{ s}^{-1}$) being lower than previously reported
184 ones (1.98 ± 0.18 to $2.39 \pm 0.30 \times 10^{-10} \text{ cm}^3 \text{ molecule}^{-1} \text{ s}^{-1}$), which may be related to the lower
185 temperature in our study and measurement uncertainty due to its rapid rate.



186

187 **Figure 1.** Plots of $\ln([\text{sulfur-VOC}]_t/[\text{sulfur-VOC}]_0)$ versus reaction time for $\bullet\text{OH}$ -initiated decay of 1,2-
188 ethanedithiol ($\text{HS}(\text{CH}_2)_2\text{SH}$), 1,3-propanedithiol ($\text{HS}(\text{CH}_2)_3\text{SH}$), dimethyl sulfide (CH_3SCH_3),
189 bis(methylthio)methane ($\text{CH}_3\text{SCH}_2\text{SCH}_3$), trimethylene sulfide ($\text{C}_3\text{H}_6\text{S}$), and 1,3-dithiolane ($\text{C}_3\text{H}_6\text{S}_2$).

190



191

Table 2. Inter-comparison of our results with other measurements of reaction rates for 10 sulfur-VOCs with •OH.

Species	sulfur-VOCs	Formulae	$k \times 10^{11}$ ($\text{cm}^3 \text{molecule}^{-1} \text{s}^{-1}$)	T (K)	p (Pa)	Buffer gas	Technique ^a	Reference	
Monothiol	ethanethiol	$\text{CH}_3\text{CH}_2\text{SH}$	3.89 ± 0.57	298	1.01×10^5	air	CP-GC	Ref. (Wang et al., 2008)	
			4.50 ± 0.50	300	1.01×10^5	N_2	CP-GC	Ref. (Barnes et al., 1986)	
	1-propanethiol	$\text{CH}_3\text{CH}_2\text{CH}_2\text{SH}$	4.21 ± 0.32	298	1.0×10^4	Ar	FP-RF	Ref. (Wine et al., 1984)	
			4.44 ± 0.10	291 ± 1	1.01×10^5	air	Vocus-PTR	this work	
	2-propanethiol	$(\text{CH}_3)_2\text{CHSH}$	5.30 ± 0.60	300	1.01×10^5	N_2	CP-GC	Ref. (Barnes et al., 1986)	
			4.59	298	1.0×10^4	Ar	FP-RF	Ref. (Wine et al., 1984)	
			4.51 ± 0.14	291 ± 1	1.01×10^5	air	Vocus-PTR	this work	
Dithiol	1,2-ethanedithiol	$\text{HS}(\text{CH}_2)_2\text{SH}$	3.90 ± 0.40	300	1.01×10^5	N_2	CP-GC	Ref. (Barnes et al., 1986)	
			4.24	298	1.0×10^4	Ar	FP-RF	Ref. (Wine et al., 1984)	
			4.68 ± 0.11	291 ± 1	1.01×10^5	air	Vocus-PTR	this work	
Acyclic sulfide	1,3-propanedithiol	$\text{HS}(\text{CH}_2)_3\text{SH}$	29.88 ± 1.02	291 ± 1	1.01×10^5	air	Vocus-PTR	this work	
			8.46 ± 0.53	291 ± 1	1.01×10^5	air	Vocus-PTR	Ref. (Wang et al., 2011)	
			1.50 ± 0.29	297	1.01×10^5	air	GC-FID	Ref. (Oksadath-Mansilla et al., 2008)	
Cyclic sulfide	bis(methylthio)methane	$\text{CH}_3\text{SCH}_2\text{SCH}_3$	1.16 ± 0.42	298	1.01×10^5	air	RK-FTIR	Ref. (Wang et al., 2008)	
			1.46 ± 0.36	298	1.01×10^5	air	CP-GC	this work	
	trimethylene sulfide	$\text{C}_3\text{H}_6\text{S}_2$	1.54 ± 0.04	291 ± 1	1.01×10^5	air	Vocus-PTR	this work	
			1.49 ± 0.11	291 ± 1	1.01×10^5	air	Vocus-PTR	this work	
	1,3-dithiolane	$\text{C}_3\text{H}_6\text{S}_2$	11.53 ± 0.21	291 ± 1	1.01×10^5	air	Vocus-PTR	this work	
			6.11 ± 0.13	291 ± 1	1.01×10^5	air	Vocus-PTR	this work	
	dimethyl disulfide	$\text{CH}_3\text{S}_2\text{CH}_3$	23.90 ± 3.00	297	1466	N_2	HPL-LIF	Ref. (Abhatt et al., 1992)	
			19.80 ± 1.80	298	6666-26664	Ar	FP-RF	Ref. (Wine et al., 1981)	
				22.30 ± 8.00	298	1.01×10^5	air	CP-GC	Ref. (Cox and Sheppard, 1980)
				10.26 ± 0.20	291 ± 1	1.01×10^5	air	Vocus-PTR	this work

9

193

^aCP: Continuous Photolysis; GC: Gas Chromatography; FP: Flash Photolysis; RF: Resonance Fluorescence; FID: Flame Ionization Detection; RK: Rapid Kinetic; FTIR: Fourier

194

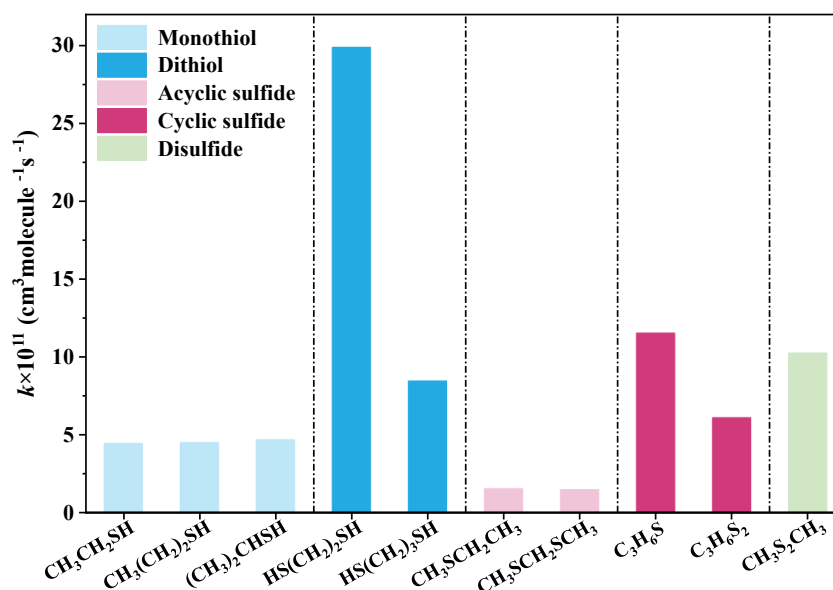
Transform Infrared Spectroscopy; HPL: High Pressure Fast; LIF: Laser Induced Fluorescence



195 Based on these measured rate constants, molecular structure-reactivity relationships can be
196 observed among the investigated sulfur-VOCs, as illustrated in Figure 2. Sulfur-VOCs containing
197 S-H functional groups, such as thiols and dithiols, generally react more rapidly with •OH than
198 acyclic sulfides, reflecting the high reactivity of the S-H bond toward H-abstraction by •OH. For
199 dithiols, the presence of two S-H groups provides multiple accessible H-abstraction sites for •OH
200 and thus can enhance the overall reactivity. The higher rate observed for 1,2-ethanedithiol
201 (HS(CH₂)₂SH) relative to 1,3-propanedithiol (HS(CH₂)₃SH) may further hint the importance of
202 vicinal configuration of the two S-H groups.

203 Acyclic sulfides, which lack S-H functional groups, typically exhibit lower reaction rates because
204 their oxidation by •OH proceeds mainly through abstraction from α -C-H bonds, which are less
205 reactive than S-H bonds. Notably, disulfides react faster than acyclic sulfides despite also lacking
206 S-H groups, highlighting the activating role of the S-S bond in facilitating radical formation during
207 the initial •OH attack. Bis(methylthio)methane (CH₃SCH₂SCH₃), although containing two sulfur
208 atoms, behaves kinetically more like an acyclic sulfide, indicating that the presence of an S-S bond
209 is a key structural factor enhancing reactivity.

210 Cyclic sulfides display intermediate reactivity, with reaction rates that are higher than those of
211 acyclic sulfides. This behavior is likely influenced by ring strain, owing to stronger ring strain, such
212 as that in trimethylene sulfide (C₃H₆S), can enhance reactivity by lowering the barrier for H-
213 abstraction. Overall, the reaction rates of sulfur-VOCs with •OH increase when molecules
214 containing more reactive S-H, S-S bond and cyclic structure, whereas compounds are limited
215 primarily to H-abstraction from α -C-H bonds generally react more slowly.



216

217

Figure 2. Reaction rates of 10 sulfur-VOCs with •OH, divided by their functional groups.

218

3.2 Formation of multi-sulfur products

219

During our chamber experiments, many multi-sulfur products which contain 2 sulfur atoms in their chemical formulas were detected by nitrate-CI-LToF-MS (Table S3). The formation pathways of multi-sulfur products from •OH-initiated oxidation of 11 selected sulfur-VOCs under NO_x-free conditions were investigated. The 11 sulfur-VOCs examined here comprise 5 thiols (CH₃CH₂SH, CH₃(CH₂)₂SH, (CH₃)₂CHSH, HS(CH₂)₂SH, HS(CH₂)₃SH), 3 acyclic sulfides (CH₃SCH₃, CH₃CH₂SCH₃, CH₃SCH₂SCH₃), 2 cyclic sulfides (C₃H₆S, C₃H₆S₂) and 1 disulfide (CH₃S₂CH₃). Among them, to exhibit the formation pathways of multi-sulfur products, DMS and HS(CH₂)₂SH are adopted as representative compounds for acyclic sulfides and thiols, respectively, whereas DMDS is treated as a representative compound for disulfide.

228

The reactions between DMS and •OH primarily proceed via two competing pathways (Scheme 1). One is that •OH adds to sulfur atom to form CH₃S•(OH)CH₃. Another is that •OH abstracts H-atom from the methyl group to generate the CH₃SCH₂•. These primary radicals subsequently react with O₂ to form a series of sulfur-containing RO₂• (i.e., CH₃SOO•, CH₃S(O)OO•, and CH₃S(O)₂OO•) (Berndt et al., 2023; Goss and Kroll, 2023; Shen et al., 2022). Notably, under NO_x-free conditions, these sulfur-containing RO₂• tend to undergo bimolecular reactions with another R'O₂• and HO₂•, instead of termination by NO_x. Under NO_x-free conditions, the fate of sulfur-RO₂• is primarily determined by the competition between RO₂• + HO₂• and RO₂• + R'O₂• reactions. Box-model simulation shows that RO₂• + R'O₂• reactions initially dominate the reaction system, but their relative contribution gradually decreases to approximately 50% as the reaction proceeds (Text S6;

237



238 Figure S7 and S8). This sustained and substantial participation of $\text{RO}_2\bullet + \text{R}'\text{O}_2\bullet$ underscores its
239 critical role in generating the observed multi-sulfur products. Based on the detection by nitrate-Cl-
240 LTof-MS, various multi-sulfur bimolecular products (e.g., $\text{C}_2\text{H}_6\text{O}_4\text{S}_2$ and $\text{C}_2\text{H}_6\text{O}_5\text{S}_2$) resulting from
241 $\text{RO}_2\bullet\text{-R}'\text{O}_2\bullet$ reactions were identified (Figure S6). Among these, $\text{C}_2\text{H}_6\text{O}_4\text{S}_2$ may originate from the
242 bimolecular reaction of $\text{CH}_3\text{SOO}\bullet$ with $\text{CH}_3\text{S}(\text{O})_2\text{OO}\bullet$ or the self-polymerization of $\text{CH}_3\text{S}(\text{O})\text{OO}\bullet$,
243 while $\text{C}_2\text{H}_6\text{O}_5\text{S}_2$ may be formed by the bimolecular reaction between $\text{CH}_3\text{S}(\text{O})_2\text{OO}\bullet$ and
244 $\text{CH}_3\text{S}(\text{O})\text{OO}\bullet$ (Scheme 1).

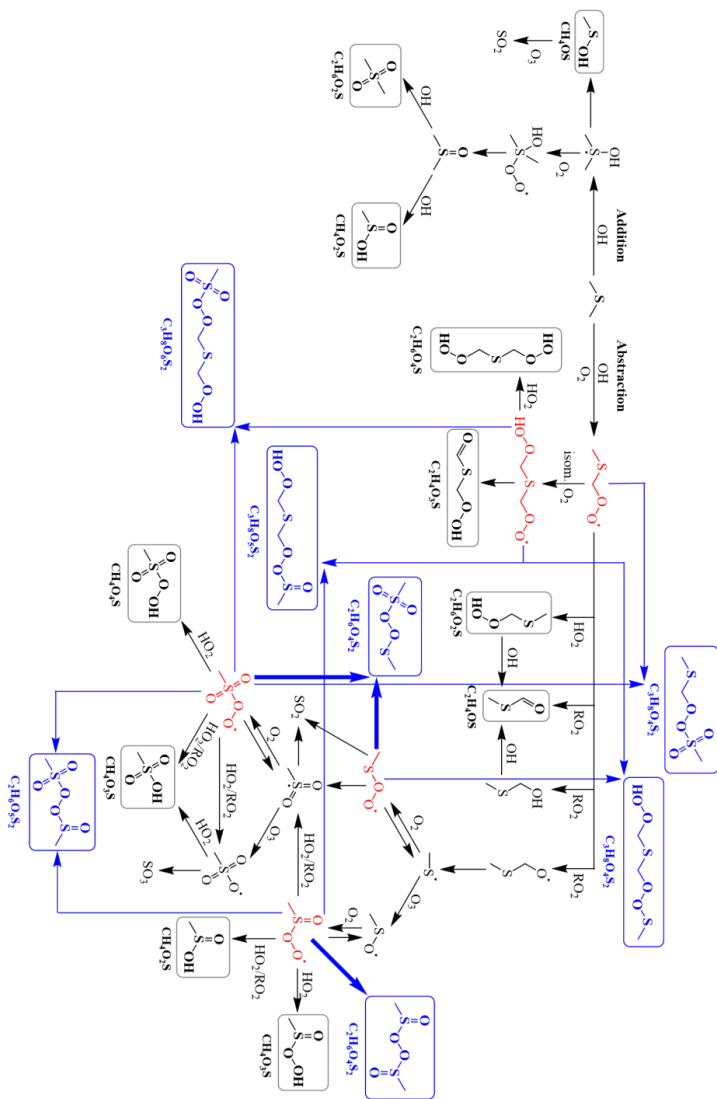
245 Previous studies on the $\bullet\text{OH}$ -initiated oxidation of DMS have extensively investigated the
246 formation and fate of sulfur- $\text{RO}_2\bullet$, and have highlighted the potential importance of $\text{RO}_2\bullet\text{-R}'\text{O}_2\bullet$
247 reactions, particularly under low- NO_x or NO_x -free conditions (Barnes et al., 2006; Ye et al., 2022).
248 However, direct molecular-level identification of multi-sulfur products has been very limited in
249 earlier studies. Most previous investigations mainly focused on major oxidation products such as
250 $\text{C}_2\text{H}_6\text{OS}$ (dimethyl sulfoxide), $\text{C}_2\text{H}_6\text{O}_2\text{S}$ (dimethyl sulfone), CH_4SO_3 , and SO_2 , rather than explicit
251 characterization of individual bimolecular products from $\text{RO}_2\bullet\text{-R}'\text{O}_2\bullet$ chemistry (Chen et al., 2023;
252 Hatakeyama et al., 1982). Self- and cross-reactions of $\text{RO}_2\bullet$ are known to produce organic peroxides
253 (ROOR') and multimeric products, and such pathways have been experimentally confirmed for a
254 variety of alkyl peroxy radicals (Cho et al., 2023; Nozière, 2025; Orlando and Tyndall, 2012). In
255 addition, studies on highly oxygenated organic molecules (HOMs) formation from biogenic VOC
256 oxidation have demonstrated that $\text{RO}_2\bullet\text{-R}'\text{O}_2\bullet$ reactions can lead to complex, multifunctional
257 products that are efficiently detected using nitrate-CIMS (Bianchi et al., 2019; Ehn et al., 2014; Gao
258 et al., 2023). Nevertheless, there have been no previous reports explicitly identifying molecular
259 formulas such as $\text{C}_2\text{H}_6\text{O}_4\text{S}_2$ and $\text{C}_2\text{H}_6\text{O}_5\text{S}_2$ as products of $\text{RO}_2\bullet\text{-R}'\text{O}_2\bullet$ reactions in the atmospheric
260 oxidation of sulfur-VOCs. The formation of these multi-sulfur products can likely be favored by
261 low- NO_x and NO_x -free experimental conditions, which can prolong the lifetime of sulfur-containing
262 $\text{RO}_2\bullet$ and favor their bimolecular reactions.

263 As shown in Scheme S1, the $\bullet\text{OH}$ -initiated oxidation of DMDS follows a reaction framework
264 similar to that of sulfides. Cleavage of the S-S bond leads to the formation of sulfur-centered radical
265 intermediates which are analogous to those generated from acyclic sulfides. Among the multi-sulfur
266 products detected from the $\bullet\text{OH}$ -initiated oxidation of DMDS, $\text{C}_2\text{H}_6\text{O}_4\text{S}_2$ was identified under the
267 present experimental conditions, and its formation is also derived from $\text{RO}_2\bullet\text{-R}'\text{O}_2\bullet$ bimolecular
268 reactions inferred for the DMS oxidation system.

269



270 **Scheme 1.** Scheme of the reaction pathways of DMS (CH_3SCH_3) with $\cdot\text{OH}$. Gray boxes denote mono-sulfur oxygenated organic products detected by Vocals-PTR-LToF-MS
 271 and nitrate-Cl-LToF-MS. Blue boxes indicate multi-sulfur products detected by nitrate-Cl-LToF-MS and these multi-sulfur products are presumably generated by the red-
 272 labeled sulfur-containing RO_2 radicals via bimolecular reactions. The bold blue arrows highlight the potential dominant pathways leading to the abundant multi-sulfur products.



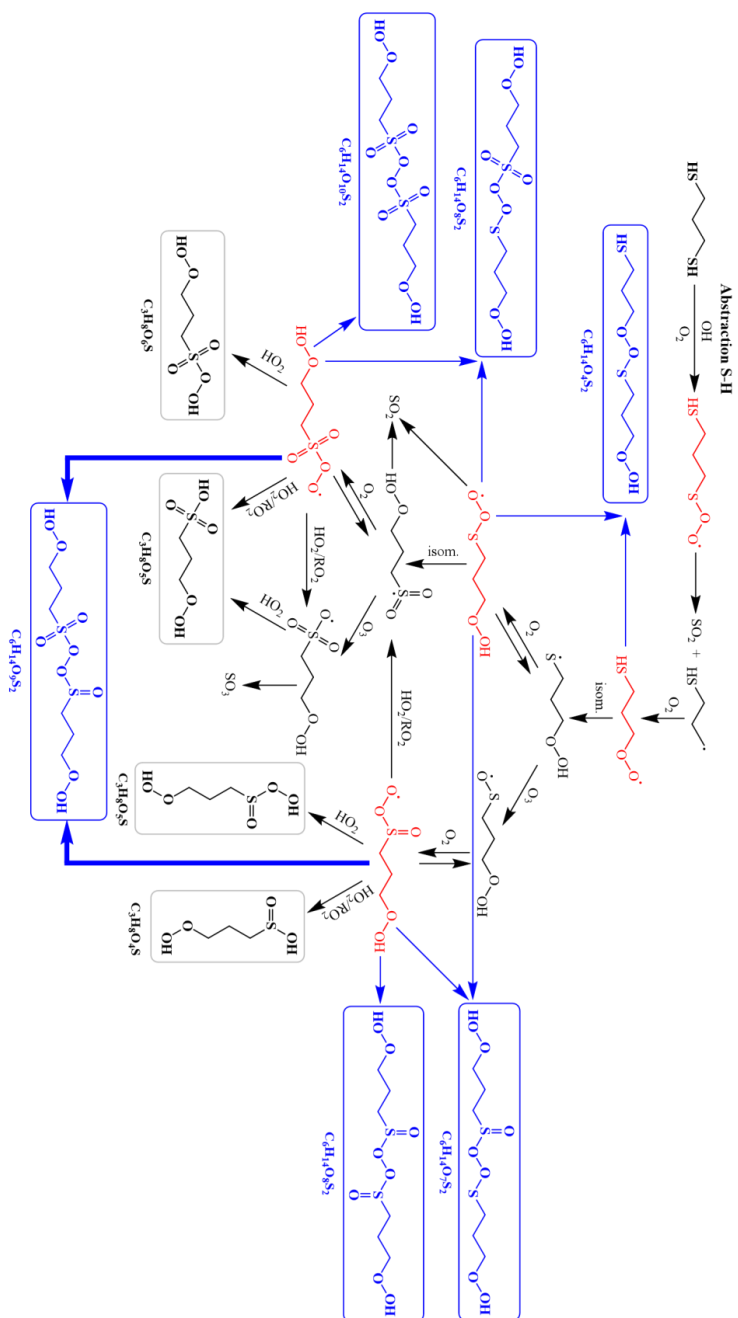


273 For thiols, the reactions between $\text{HS}(\text{CH}_2)_3\text{SH}$ and $\bullet\text{OH}$ are initiated predominantly by H-
274 abstraction from the S-H group (Scheme 2), forming the sulfur-centered radical ($\text{HS}(\text{CH}_2)_3\text{S}\bullet$)
275 (Berndt et al., 2023; Douroudgari et al., 2020; Mai et al., 2020). Subsequent reactions lead to the
276 formation of a few sulfur-containing $\text{RO}_2\bullet$ intermediates, including $\text{HS}(\text{CH}_2)_3\text{OO}\bullet$,
277 $\text{HOO}(\text{CH}_2)_3\text{SOO}\bullet$, and $\text{HOO}(\text{CH}_2)_3\text{S}(\text{O})_2\text{OO}\bullet$. Compared to $\text{RO}_2\bullet$ derived from acyclic sulfides and
278 disulfides, thiol-derived $\text{RO}_2\bullet$ exhibit more structurally diverse, enabling more bimolecular reaction
279 pathways. As a result, more multi-sulfur products were identified (Figure S10), including $\text{C}_6\text{H}_{14}\text{O}_8\text{S}_2$,
280 $\text{C}_6\text{H}_{14}\text{O}_9\text{S}_2$, $\text{C}_6\text{H}_{14}\text{O}_{10}\text{S}_2$, etc. Plausible formation pathways for these multi-sulfur products are
281 illustrated in Scheme 2. Specifically, $\text{C}_6\text{H}_{14}\text{O}_9\text{S}_2$ can originate from the bimolecular reaction of
282 $\text{HOO}(\text{CH}_2)_3\text{S}(\text{O})_2\text{OO}\bullet$ with $\text{HOO}(\text{CH}_2)_3\text{S}(\text{O})\text{OO}\bullet$. The formation pathways of $\text{C}_6\text{H}_{14}\text{O}_8\text{S}_2$ and
283 $\text{C}_6\text{H}_{14}\text{O}_{10}\text{S}_2$ are similar with $\text{C}_6\text{H}_{14}\text{O}_9\text{S}_2$. In addition, multi-sulfur products were also detected for
284 other investigated sulfur-VOCs (Figures S9 and S11-S13). Although acyclic sulfides and disulfides
285 are structurally distinct, the reaction pathways presented above indicates that their $\bullet\text{OH}$ -initiated
286 oxidation proceeds through similar sulfur-centered radical intermediates and subsequent reactions
287 of sulfur- $\text{RO}_2\bullet$.
288



289
290
291

Scheme 2. Scheme of the reaction pathways of HS(CH₂)₅SH with •OH. Gray boxes denote mono-sulfur oxygenated organic products detected by Vocou-PTR-LToF-MS and nitrate-Cl-LToF-MS. Blue boxes indicate multi-sulfur products detected by nitrate-Cl-LToF-MS and these multi-sulfur products are presumably generated by the red-labeled sulfur-containing RO₂ radicals via bimolecular reactions. The bold blue arrows highlight the potential dominant pathways leading to the abundant multi-sulfur products

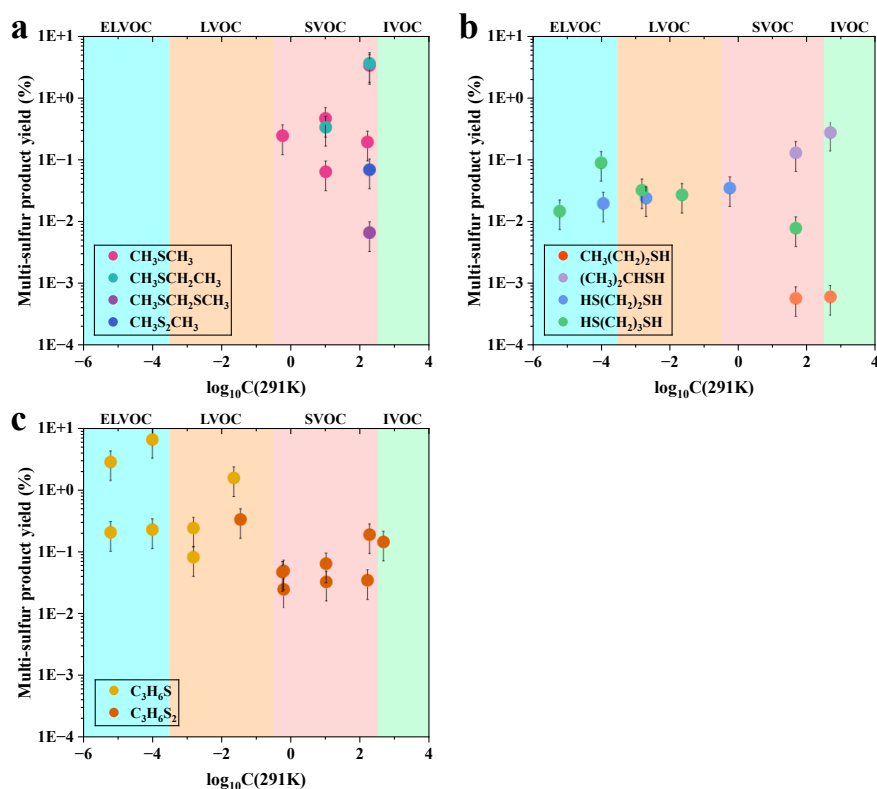




292 To evaluate the yields and volatility distributions of these multi-sulfur products, Figure 3
293 summarizes the estimated volatility distributions and formation yields from the •OH-initiated
294 oxidation of 10 sulfur-VOCs except for ethanethiol. No multi-sulfur products were detected for
295 ethanethiol, suggesting that their formation was either negligible or that the resulting concentrations
296 were below the detection limit of the nitrate-CI-LToF-MS. The volatilities were estimated using the
297 parameterization proposed by Li et al., 2016. Overall, the total yields of multi-sulfur products varied
298 substantially among the 10 sulfur-VOCs, ranging from 0.001% to 11.73% (Table S3), indicating a
299 strong dependence on precursor structure and sulfur functionality.

300 Among all investigated compounds, trimethylene sulfide (C_3H_6S) exhibited the highest total yield
301 (11.73%), suggesting its highly efficient formation of multi-sulfur products. In contrast, several thiol
302 systems and certain acyclic sulfides produced only trace amounts of multi-sulfur products, with total
303 yields below 0.1%. Acyclic sulfides and disulfide systems (e.g., DMS) predominantly generated
304 semi-volatile organic compounds (SVOCs), with total multi-sulfur yields generally below ~4%. In
305 comparison, cyclic sulfides displayed more diverse volatility distributions. For C_3H_6S , multi-sulfur
306 products extended into the low-volatility organic compounds (LVOCs) and extremely low-volatility
307 organic compounds (ELVOCs) regimes, with a significant fraction of the total yield residing in these
308 low-volatility classes. By contrast, 1,3-dithiolane ($C_3H_6S_2$) mainly produced SVOCs-range multi-
309 sulfur products, and individual species yields remained below ~0.4%, despite a moderate summed
310 yield. Thiols (e.g., $HS(CH_2)_3SH$) exhibited a distinct pattern: although their oxidation generated
311 products extending into the LVOCs and ELVOCs regimes, the overall formation efficiency was low,
312 with total yields ranging from 0.001% to 0.40%. This suggests that structural factors, such as the
313 position and number of -SH groups, may influence both $RO_2\bullet$ reactivity and multi-sulfur product
314 formation efficiency. The presence of LVOCs and ELVOCs multi-sulfur products, particularly for
315 cyclic sulfides, implies a potential role in secondary organic aerosol formation and particle growth.

316 It should be noted that the semi-quantification of these multi-sulfur products is based on the
317 calibration factor of gaseous sulfuric acid (H_2SO_4) (Text S2). It was assumed that the ionization
318 efficiency of H_2SO_4 towards the reagent ions ($(HNO_3)_nNO_3^-$, $n=0, 1$ and 2) is the same as that of
319 multi-sulfur products. As a result, the reported yields may have an additional uncertainty because of
320 ionization efficiency difference between H_2SO_4 and multi-sulfur products towards the reagent ions.
321



322

323 **Figure 3.** Volatility ($\log_{10} C^*$, at 291 K) versus the yield (%) of multi-sulfur products formed from the
 324 $\bullet\text{OH}$ -initiated oxidation of sulfur-VOCs. (a) acyclic sulfides and disulfide: CH_3SCH_3 , $\text{CH}_3\text{SCH}_2\text{CH}_3$,
 325 $\text{CH}_3\text{SCH}_2\text{SCH}_3$ and $\text{CH}_3\text{S}_2\text{CH}_3$; (b) thiols: $\text{CH}_3(\text{CH}_2)_2\text{SH}$, $(\text{CH}_3)_2\text{CHSH}$, $\text{HS}(\text{CH}_2)_2\text{SH}$, and $\text{HS}(\text{CH}_2)_3\text{SH}$;
 326 (c) cyclic sulfides: $\text{C}_3\text{H}_6\text{S}$, $\text{C}_3\text{H}_6\text{S}_2$. The volatility ranges were divided into ELVOCs, LVOCs, SVOCs
 327 and IVOCs (intermediate volatile organic compounds). Error bars represent an estimated uncertainty of
 328 approximately $\pm 50\%$, primarily arising from the use of calibration factor of gaseous H_2SO_4 .

329 3.3 Identification and atmospheric oxidation of sulfur-VOCs and other VOCs emitted from 330 freshwater algae

331 As shown in Figure 4a, the emitted VOCs from freshwater algae were measured by Vocus-PTR-
 332 LToF-MS and 240 compounds in total were identified, including 143 CHO species, 43 CH species,
 333 20 sulfur-VOCs, and 34 other VOCs. High-resolution peak fittings for the assigned sulfur-VOCs
 334 were shown in Figure S15. The molecular formulas and mixing ratios of 20 sulfur-VOCs are
 335 summarized in Table S4 and Figure 4b.

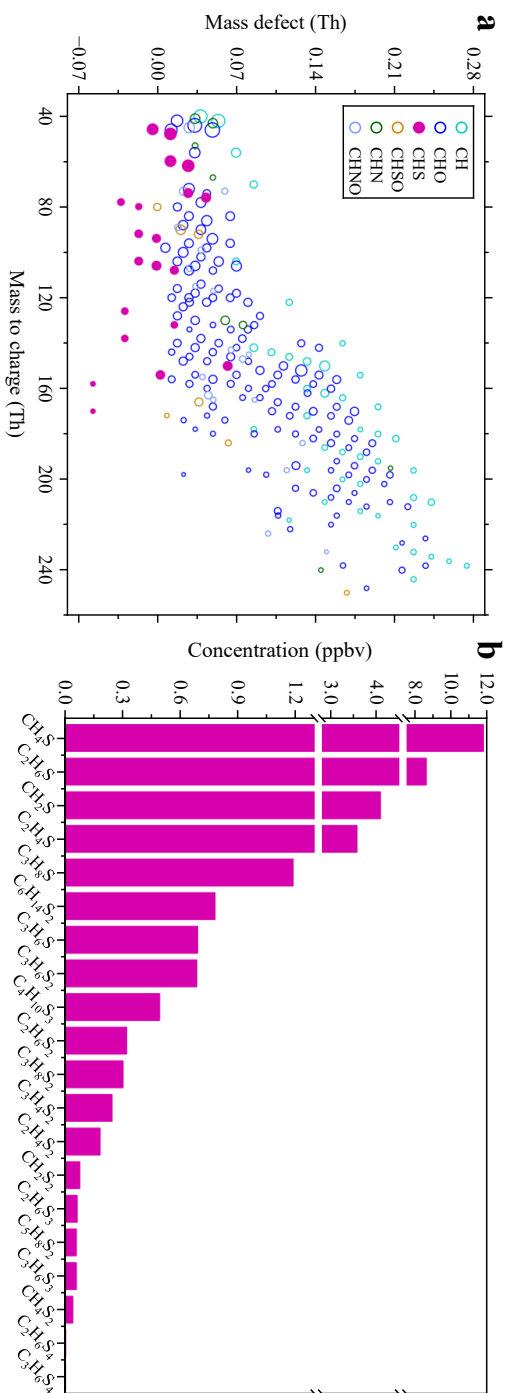
336 Under the specific treatment conditions (see Section 2.2), absolute mixing ratios of emitted VOCs
 337 spanned over three orders of magnitude, ranging from 0.01 to 11.77 ppbv. Among the 20 identified
 338 sulfur-VOCs, 6 monosulfur species were detected and they are dominated ones. Specifically, CH_4S



339 reached the highest level (11.77 ppbv), followed by C_2H_6S (8.60 ppbv), CH_2S (4.09 ppbv), and
340 C_2H_4S (3.57 ppbv), while the remaining monosulfur species were present at sub-ppbv levels. 9
341 disulfur species were identified with generally lower abundances, spanning from 0.04 to 0.78 ppbv,
342 with $C_6H_{14}S_2$ (0.78 ppbv) and $C_3H_6S_2$ (0.69 ppbv) representing the most abundant disulfur species.
343 3 trisulfur species were detected at similarly low levels, ranging from 0.06 to 0.50 ppbv, with
344 $C_4H_{10}S_3$ showing the highest mixing ratio within this group. In contrast, 2 tetrasulfur species were
345 the least abundant, with mixing ratios decreasing to ~ 0.01 ppbv for $C_2H_6S_4$ and $C_3H_6S_4$. Overall, a
346 clear and systematic decrease in mixing ratios was observed with increasing sulfur number.

347 In addition, removal of most algae by filtration led to a remarkable decrease in sulfur-VOC signals
348 (Figure S16), supporting that these sulfur-VOCs were primarily associated with freshwater algae.
349 Although only molecular formulas rather than structures could be assigned, the results still provide
350 a comprehensive inventory of freshwater algae-emitted sulfur-VOCs. Notably, the molecular
351 formulas of sulfur-VOCs targeted in our chamber study were also present in the list of sulfur-VOCs
352 emitted from freshwater algae. Although Vocus-PTR-LToF-MS measurements constrain molecular
353 formulas rather than isomer-specific structures, the co-occurrence of these formula families in algal
354 emissions supports the atmospheric relevance of the structure-resolved kinetics and oxidation
355 mechanisms derived from our chamber experiments.

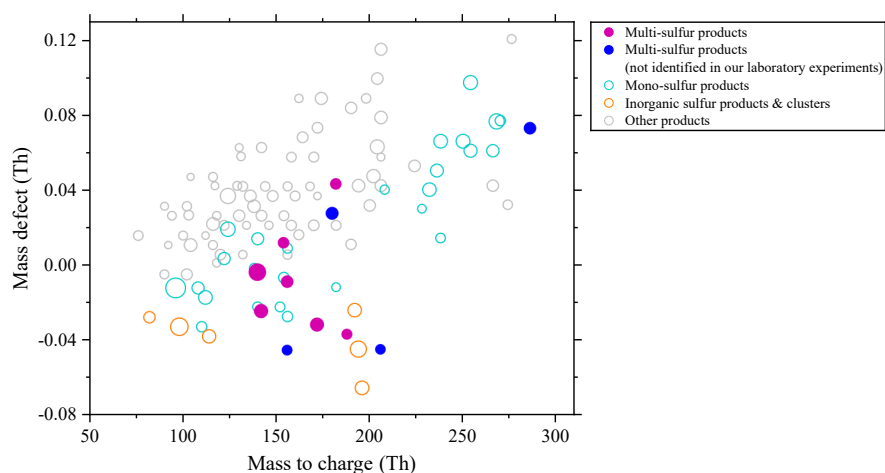
356



357
 358 **Figure 4.** (a) Mass defect plot of emitted VOCs from freshwater algae measured by Vocous-PTR-LToF-MS, with data points color-coded by elemental composition (CH, CHO,
 359 CHS, CHSO, CHN, and CHNO) and marker size scaled to signal intensity. (b) Mixing ratios of the 20 sulfur-VOCs detected from the algal emissions



360 In subsequent atmospheric oxidation experiments of these emitted VOCs including sulfur-VOCs,
361 our chamber was maintained under NO_x-free conditions, hence the termination of RO₂• by NO_x was
362 suppressed and bimolecular reactions of RO₂• were favored. Approximately 110 oxidation products
363 were identified using nitrate-CI-LToF-MS, including dozens of mono-sulfur organic compounds, a
364 few inorganic sulfur-containing species (e.g., H₂SO₄ and its clusters), and 11 multi-sulfur products
365 (Figure 5 and Table S5). Among 11 multi-sulfur products, 7 of them could be inferred from our
366 selected sulfur-VOCs chamber simulation experiments and their high-resolution peak fitting plots
367 were also shown in Figure S17. Additionally, 4 multi-sulfur products could not be reproduced from
368 our chamber simulation experiments (Figure S18). These experimental results not only confirm that
369 multi-sulfur products can be formed from bimolecular reactions of sulfur-RO₂•, but also promote
370 the understanding of atmospheric chemical processes of sulfur-VOCs in ambient air (especially in
371 low NO_x environments). Notably, the detection of H₂SO₄ and its clusters known as precursors for
372 new particle formation suggests that the oxidation of algae-emitted sulfur-VOCs can contribute to
373 secondary particle formation. However, due to the complex composition of algae-derived sulfur-
374 VOCs, specific formation pathways of these multi-sulfur products need to be further elucidated.



375
376 **Figure 5.** Mass defect plot of oxidation products formed from the •OH-initiated oxidation of algae-
377 emitted VOCs. Multi-sulfur products shown in deep purple represent species whose molecular formulas
378 were also identified in our chamber simulation experiments of the selected sulfur-VOCs, whereas those
379 shown in dark blue represent multi-sulfur products whose corresponding molecular formulas were not
380 identified in our chamber experiments. Marker size is proportional to the corresponding signal intensity.
381

382 Although the oxidation experiments were conducted under NO_x-free conditions, such chemical
383 regimes are still representative of atmospherically relevant environments characterized by low NO_x



384 levels and strong biogenic emissions (e.g., inland eutrophic lakes, remote marine boundary layer
385 and polar regions). In these environments, NO_x concentrations are typically very low and $\text{RO}_2\bullet$
386 termination by NO_x is strongly suppressed (Berresheim et al., 1998; Novak et al., 2022; Read et al.,
387 2008; Steinke et al., 2018). Field observations in these environments have reported sulfur-VOCs
388 such as DMS and methanethiol at dozens to hundreds of pptv levels (Berresheim et al., 1998; Novak
389 et al., 2022; Read et al., 2008). Therefore, multi-sulfur products derived from $\text{RO}_2\bullet\text{-R}'\text{O}_2\bullet$
390 bimolecular reactions during atmospheric oxidation of sulfur-VOCs may contribute SOA formation
391 in these environments. While the quantitative contribution of sulfur-VOCs-derived multi-sulfur
392 products to SOA formation remains uncertain, the present results only highlight the detection and
393 formation pathways of multi-sulfur products from atmospheric oxidation of sulfur-VOCs.

394 **4 Conclusions**

395 This study provides an integrated understanding of kinetics and formation pathways of multi-
396 sulfur products of $\bullet\text{OH}$ -initiated oxidation of a series of selected sulfur-VOCs with different
397 functional groups. Reaction rate constants determined for these sulfur-VOCs reveal clear structure-
398 reactivity relationships and sulfur- $\text{RO}_2\bullet$ can undergo bimolecular reactions under low NO_x , leading
399 to the formation of multi-sulfur products with distinct volatility characteristics. Acyclic sulfides and
400 disulfides mainly produce semi-volatile multi-sulfur products with relatively higher yields, whereas
401 thiols (particularly dithiols) favor the formation of more highly oxygenated, low-volatility products
402 that may promote SOA formation. Furthermore, the selected sulfur-VOCs were also observed from
403 the emission of freshwater algae and some of multi-sulfur products derived from our chamber
404 simulation experiments of selected sulfur-VOCs were also identified from $\bullet\text{OH}$ -initiated oxidation
405 of VOCs emitted from freshwater algae. These results together further confirm the atmospheric
406 relevance of these selected sulfur-VOCs and the sulfur- $\text{RO}_2\bullet$ chemistry leading to the formation of
407 multi-sulfur products.

408 Biogenic sulfur-VOCs could have increased significance in the context of ongoing changes in the
409 atmospheric sulfur budget. Anthropogenic SO_2 emissions have been declining worldwide, reducing
410 the dominance of the traditional gaseous H_2SO_4 formation pathway from anthropogenic SO_2 in
411 atmospheric sulfur cycling. Instead, the oxidation of biogenic sulfur-VOCs is likely to become an
412 increasingly important source for gaseous H_2SO_4 and particulate sulfate, particularly in low- NO_x
413 environments. The formation of low-volatility multi-sulfur products via sulfur- $\text{RO}_2\bullet$ bimolecular
414 reactions highlight an additional pathway by which sulfur-VOCs can contribute to SOA formation.
415 Overall, this study underscores the growing role of biogenic sulfur-VOCs in atmospheric sulfur
416 budget and highlights the necessity of explicitly considering the atmospheric chemistry of sulfur-
417 VOCs in atmospheric models.

418



419 **Data availability.** The data used to support the conclusions in this study are available at a public
420 data repository of Zenodo via <https://doi.org/10.5281/zenodo.18923240>. Additional data related to
421 this paper can be requested from the authors (lei_yao@fudan.edu.cn).

422

423 **Author contributions.** L.Y. conceived and designed this study and revised the manuscript. X.R.
424 conducted the experiments, performed data analysis, and prepared the manuscript with contributions
425 from all co-authors. C.L. assisted in designing the experiments. C.A. and G.Y. assisted with data
426 collection. J.L.S, R.L.C., D. R. Worsnop, and L.W. interpreted the results and revised the manuscript.

427

428 **Competing interests.** The contact author has declared that none of the authors has any competing
429 interests.

430

431 **Acknowledgements.** This research was supported by the National Key Research and Development
432 Program of China (2022YFC3704100) and the National Natural Science Foundation of China
433 (22376031).

434



References

- Abbatt, J. P. D., Fenter, F. F., and Anderson, J. G.: High-pressure discharge flow kinetics study of hydroxyl + dimethyl sulfide, dimethyl disulfide .fwdarw. products from 297 to 368 K, *J. Phys. Chem.*, 96, 1780–1785, <https://doi.org/10.1021/j100183a053>, 1992.
- Atkinson, R., Baulch, D. L., Cox, R. A., Crowley, J. N., Hampson, R. F., Hynes, R. G., Jenkin, M. E., Rossi, M. J., and Troe, J.: Evaluated kinetic and photochemical data for atmospheric chemistry: Volume I - gas phase reactions of O_x, HO_x, NO_x and SO_x species, *Atmos. Chem. Phys.*, 4, 1461–1738, <https://doi.org/10.5194/acp-4-1461-2004>, 2004.
- Bao, Q., Wu, A., Lu, J., Jiang, L., and Shen, Q.: Analysis of Three Dimethyl Sulfides in Freshwater Lakes Using Headspace Solid-Phase Microextraction-Gas Chromatography with Flame Photometric Detection, *Atmosphere*, 15, 484, <https://doi.org/10.3390/atmos15040484>, 2024.
- Barnes, I., Bastian, V., Becker, K. H., Fink, E. H., and Nelsen, W.: Oxidation of sulphur compounds in the atmosphere: I. Rate constants of OH radical reactions with sulphur dioxide, hydrogen sulphide, aliphatic thiols and thiophenol, *J. Atmos. Chem.*, 4, 445–466, <https://doi.org/10.1007/bf00053845>, 1986.
- Barnes, I., Hjorth, J., and Mihalopoulos, N.: Dimethyl Sulfide and Dimethyl Sulfoxide and Their Oxidation in the Atmosphere, *Chem. Rev.*, 106, 940–975, <https://doi.org/10.1021/cr020529t>, 2006.
- Berndt, T., Hoffmann, E. H., Tilgner, A., Stratmann, F., and Herrmann, H.: Direct sulfuric acid formation from the gas-phase oxidation of reduced-sulfur compounds, *Nat. Commun.*, 14, 4849, <https://doi.org/10.1038/s41467-023-40586-2>, 2023.
- Berndt, T., Hoffmann, E. H., Tilgner, A., and Herrmann, H.: Gas-Phase Formation of Sulfurous Acid (H₂SO₃) in the Atmosphere, *Angew. Chem. Int. Ed.*, e202405572, <https://doi.org/10.1002/anie.202405572>, 2024.
- Berresheim, H., Huey, J. W., Thorn, R. P., Eisele, F. L., Tanner, D. J., and Jefferson, A.: Measurements of dimethyl sulfide, dimethyl sulfoxide, dimethyl sulfone, and aerosol ions at Palmer Station, Antarctica, *J. Geophys. Res.: Atmos.*, 103, 1629–1637, <https://doi.org/10.1029/97jd00695>, 1998.
- Bianchi, F., Kurtén, T., Riva, M., Mohr, C., Rissanen, M. P., Roldin, P., Berndt, T., Crouse, J. D., Wennberg, P. O., Mentel, T. F., Wildt, J., Junninen, H., Jokinen, T., Kulmala, M., Worsnop, D. R., Thornton, J. A., Donahue, N., Kjaergaard, H. G., and Ehn, M.: Highly Oxygenated Organic Molecules (HOM) from Gas-Phase Autoxidation Involving Peroxy Radicals: A Key Contributor to Atmospheric Aerosol, *Chem. Rev.*, 119, 3472–3509, <https://doi.org/10.1021/acs.chemrev.8b00395>, 2019.



Chen, J., Lane, J. R., and Kjaergaard, H. G.: Reaction of Atmospherically Relevant Sulfur-Centered Radicals with RO₂ and HO₂, *J. Phys. Chem. A*, 127, 2986–2991, <https://doi.org/10.1021/acs.jpca.3c00558>, 2023.

Cho, J., Mulvihill, C. R., Klippenstein, S. J., and Sivaramakrishnan, R.: Bimolecular Peroxy Radical (RO₂) Reactions and Their Relevance in Radical Initiated Oxidation of Hydrocarbons, *J. Phys. Chem. A*, 127, 300–315, <https://doi.org/10.1021/acs.jpca.2c06960>, 2023.

Cox, R. A. and Sheppard, D.: Reactions of OH radicals with gaseous sulphur compounds, *Nature*, 284, 330–331, <https://doi.org/10.1038/284330a0>, 1980.

Cruz-Torres, A. and Galano, A.: On the Mechanism of Gas-Phase Reaction of C₁–C₃ Aliphatic Thiols + OH Radicals, *J. Phys. Chem. A*, 111, 1523–1529, <https://doi.org/10.1021/jp0673415>, 2007.

Dai, Y., Yang, S., Zhao, D., Hu, C., Xu, W., Anderson, D. M., Li, Y., Song, X.-P., Boyce, D. G., Gibson, L., Zheng, C., and Feng, L.: Coastal phytoplankton blooms expand and intensify in the 21st century, *Nature*, 615, 280–284, <https://doi.org/10.1038/s41586-023-05760-y>, 2023.

Deng, K., Huo, J., Wang, Y., Wang, L., Yin, S., Li, C., Li, Y., Yang, G., Yao, L., Fu, Q., and Wang, L.: Characteristics of atmospheric reduced-sulfur compounds at a suburban site of Shanghai, *J. Environ. Sci.*, 156, 671–683, <https://doi.org/10.1016/j.jes.2024.06.030>, 2025.

Douroudgari, H., Vahedpour, M., and Mohammadi, S.: Atmospheric reaction of methyl mercaptan with hydroxyl radical as an acid rain primary agent, *Sci. Rep.*, 10, 18081, <https://doi.org/10.1038/s41598-020-74767-6>, 2020.

Ehn, M., Thornton, J. A., Kleist, E., Sipilä, M., Junninen, H., Pullinen, I., Springer, M., Rubach, F., Tillmann, R., Lee, B., Lopez-Hilfiker, F., Andres, S., Acir, I.-H., Rissanen, M., Jokinen, T., Schobesberger, S., Kangasluoma, J., Kontkanen, J., Nieminen, T., Kurtén, T., Nielsen, L. B., Jørgensen, S., Kjaergaard, H. G., Canagaratna, M., Maso, M. D., Berndt, T., Petäjä, T., Wahner, A., Kerminen, V.-M., Kulmala, M., Worsnop, D. R., Wildt, J., and Mentel, T. F.: A large source of low-volatility secondary organic aerosol, *Nature*, 506, 476–479, <https://doi.org/10.1038/nature13032>, 2014.

Fiddes, S. L., Woodhouse, M. T., Utembe, S., Schofield, R., Alexander, S. P., Alroe, J., Chambers, S. D., Chen, Z., Cravigan, L., Dunne, E., Humphries, R. S., Johnson, G., Keywood, M. D., Lane, T. P., Miljevic, B., Omori, Y., Protat, A., Ristovski, Z., Selleck, P., Swan, H. B., Tanimoto, H., Ward, J. P., and Williams, A. G.: The contribution of coral-reef-derived dimethyl sulfide to aerosol burden over the Great Barrier Reef: a modelling study, *Atmos. Chem. Phys.*, 22, 2419–2445, <https://doi.org/10.5194/acp-22-2419-2022>, 2021.

Gao, Y., Lu, K., and Zhang, Y.: Review of technologies and their applications for the speciated detection of RO₂ radicals, *J. Environ. Sci.*, 123, 487–499, <https://doi.org/10.1016/j.jes.2022.09.028>, 2023.



Goss, M. B. and Kroll, J. H.: Chamber studies of OH + dimethyl sulfoxide and dimethyl disulfide: insights into the dimethyl sulfide oxidation mechanism, *Atmos. Chem. Phys.*, 24, 1299–1314, <https://doi.org/10.5194/acp-24-1299-2024>, 2023.

Hashemi, S. R., Saheb, V., and Hosseini, S. M. A.: Theoretical kinetic study of the reaction between dimethyl disulfide and OH radicals, *J. Sulfur Chem.*, 40, 185–194, <https://doi.org/10.1080/17415993.2018.1556274>, 2019.

Hatakeyama, S., Okuda, M., and Akimoto, H.: Formation of sulfur dioxide and methanesulfonic acid in the photooxidation of dimethyl sulfide in the air, *Geophys. Res. Lett.*, 9, 583–586, <https://doi.org/10.1029/gl009i005p00583>, 1982.

Huang, H., Xu, X., Liu, X., Han, R., Liu, J., and Wang, G.: Distributions of four taste and odor compounds in the sediment and overlying water at different ecology environment in Taihu Lake, *Sci. Rep.*, 8, 6179, <https://doi.org/10.1038/s41598-018-24564-z>, 2018.

Jernigan, C. M., Fite, C. H., Vereecken, L., Berkelhammer, M. B., Rollins, A. W., Rickly, P. S., Novelli, A., Taraborrelli, D., Holmes, C. D., and Bertram, T. H.: Efficient Production of Carbonyl Sulfide in the Low-NO_x Oxidation of Dimethyl Sulfide, *Geophys. Res. Lett.*, 49, <https://doi.org/10.1029/2021gl096838>, 2022.

Jokinen, T., Lehtipalo, K., Thakur, R. C., Ylivinkka, I., Neitola, K., Sarnela, N., Laitinen, T., Kulmala, M., Petäjä, T., and Sipilä, M.: Measurement report: Long-term measurements of aerosol precursor concentrations in the Finnish subarctic boreal forest, *Atmos. Chem. Phys.*, 22, 2237–2254, <https://doi.org/10.5194/acp-22-2237-2022>, 2022.

Kietäväinen, R., Nyssönen, M., Nuppenen-Puputti, M., and Bomberg, M.: Naturally occurring volatile organic compounds in deep bedrock groundwater, *Commun. Earth Environ.*, 6, 64, <https://doi.org/10.1038/s43247-025-02053-2>, 2025.

Kilgour, D. B., Novak, G. A., Sauer, J. S., Moore, A. N., Dinasquet, J., Amiri, S., Franklin, E. B., Mayer, K., Winter, M., Morris, C. K., Price, T., Malfatti, F., Crocker, D. R., Lee, C., Cappa, C. D., Goldstein, A. H., Prather, K. A., and Bertram, T. H.: Marine gas-phase sulfur emissions during an induced phytoplankton bloom, *Atmos. Chem. Phys.*, 22, 1601–1613, <https://doi.org/10.5194/acp-22-1601-2022>, 2021.

Li, C., Yao, L., Wang, Y., Fang, M., Chen, X., Wang, L., Li, Y., Yang, G., and Wang, L.: Formation of chlorinated organic compounds from Cl atom-initiated reactions of aromatics and their detection in suburban Shanghai, *Atmos. Chem. Phys.*, 25, 11247–11260, <https://doi.org/10.5194/acp-25-11247-2025>, 2025.

Li, Y., Pöschl, U., and Shiraiwa, M.: Molecular corridors and parameterizations of volatility in the chemical evolution of organic aerosols, *Atmos. Chem. Phys.*, 16, 3327–3344, <https://doi.org/10.5194/acp-16-3327-2016>, 2016.



- Li, Y., Gong, X., Zhao, Z., Shen, Q., and Zhang, L.: Distribution and Release of Volatile Organic Sulfur Compounds in Yangcheng Lake, Water, 14, 1199, <https://doi.org/10.3390/w14081199>, 2022.
- Lily, M., Hynniewta, S., Lv, X., Chandra, A. K., Tchinda, N. T., and Du, L.: Assessing the Isomerization of a Primary Intermediate ($\text{CH}_3\text{SCH}_2\text{O}_2\cdot$ Radical) in Dimethyl Sulfide Degradation in the Marine Boundary Layer, ACS Earth Space Chem., 7, 2129–2138, <https://doi.org/10.1021/acsearthspacechem.3c00209>, 2023.
- Liu, M., Wu, T., Zhao, X., Zan, F., Yang, G., and Miao, Y.: Cyanobacteria blooms potentially enhance volatile organic compound (VOC) emissions from a eutrophic lake: Field and experimental evidence, Environ. Res., 202, 111664, <https://doi.org/10.1016/j.envres.2021.111664>, 2021.
- Lu, X., Fan, C., Shang, J., Deng, J., and Yin, H.: Headspace solid-phase microextraction for the determination of volatile sulfur compounds in odorous hyper-eutrophic freshwater lakes using gas chromatography with flame photometric detection, Microchem. J., 104, 26–32, <https://doi.org/10.1016/j.microc.2012.04.001>, 2012.
- Mai, T. V.-T., Nguyen, H. T., and Huynh, L. K.: Kinetics of hydrogen abstraction from CH_3SH by OH radicals: An ab initio RRKM-based master equation study, Atmos. Environ., 242, 117833, <https://doi.org/10.1016/j.atmosenv.2020.117833>, 2020.
- Mynard, C., Franklin, E. B., Alroe, J., Somerville, N., Patti, A., Siems, S. T., Williams, A., Mallet, M. D., Humphries, R., and Dunne, E.: Constraining Atmospheric Methanethiol Estimates Over the Southern Ocean, Geophys. Res. Lett., 52, <https://doi.org/10.1029/2025gl116470>, 2025.
- Novak, G. A., Kilgour, D. B., Jernigan, C. M., Vermeuel, M. P., and Bertram, T. H.: Oceanic emissions of dimethyl sulfide and methanethiol and their contribution to sulfur dioxide production in the marine atmosphere, Atmos. Chem. Phys., 22, 6309–6325, <https://doi.org/10.5194/acp-22-6309-2022>, 2022.
- Nozière, B.: Trends in organic peroxide (ROOR) formation in the reactions of C_1 – C_4 alkyl peroxy radicals (RO_2) in gas, Chem. Sci., 16, 16590–16596, <https://doi.org/10.1039/d5sc03559g>, 2025.
- Oksdath-Mansilla, G., Peñeñory, A. B., Albu, M., Barnes, I., Wiesen, P., and Teruel, M. A.: $\text{CH}_3\text{CH}_2\text{SCH}_3 + \text{OH}$ radicals: temperature-dependent rate coefficient and product identification under atmospheric pressure of air, J. Phys. Org. Chem., 23, 925–930, <https://doi.org/10.1002/poc.1714>, 2010.
- Orlando, J. J. and Tyndall, G. S.: Laboratory studies of organic peroxy radical chemistry: an overview with emphasis on recent issues of atmospheric significance, Chem. Soc. Rev., 41, 6294, <https://doi.org/10.1039/c2cs35166h>, 2012.
- Qin, B., Paerl, H. W., Brookes, J. D., Liu, J., Jeppesen, E., Zhu, G., Zhang, Y., Xu, H., Shi, K., and Deng, J.: Why Lake Taihu continues to be plagued with cyanobacterial blooms through 10 years (2007–2017) efforts, Sci. Bull., 64, 354–356, <https://doi.org/10.1016/j.scib.2019.02.008>, 2019.



Read, K. A., Lewis, A. C., Bauguitte, S., Rankin, A. M., Salmon, R. A., Wolff, E. W., Saiz-Lopez, A., Bloss, W. J., Heard, D. E., Lee, J. D., and Plane, J. M. C.: DMS and MSA measurements in the Antarctic Boundary Layer: impact of BrO on MSA production, *Atmos. Chem. Phys.*, 8, 2985–2997, <https://doi.org/10.5194/acp-8-2985-2008>, 2008.

Revell, L. E., Edkins, N. J., Venugopal, A. U., Bhatti, Y. A., Kozyniak, K. M., Davy, P. K., Kuschel, G., Somervell, E., Hardacre, C., and Coulson, G.: Marine aerosol in Aotearoa New Zealand: implications for air quality, climate change and public health, *J. R. Soc. N. Zealand*, ahead-of-print, 1–23, <https://doi.org/10.1080/03036758.2024.2319753>, 2024.

Rocco, M., Dunne, E., Salignat, R., Saint-Macary, A., Peltola, M., Barthelmeß, T., Chamba, G., Barr, N., Safi, K., Marriner, A., Deppeler, S., Rose, C., Uitz, J., Harnwell, J., Engel, A., Colomb, A., Saiz-Lopez, A., Harvey, M. J., Law, C. S., and Sellegri, K.: Relating Dimethyl Sulphide and Methanethiol Fluxes to Surface Biota in the South-West Pacific Using Shipboard Air-Sea Interface Tanks, *J. Geophys. Res.: Atmos.*, 130, <https://doi.org/10.1029/2024jd041072>, 2025.

Shen, J., Scholz, W., He, X.-C., Zhou, P., Marie, G., Wang, M., Marten, R., Surdu, M., Rörup, B., Baalbaki, R., Amorim, A., Ataei, F., Bell, D. M., Bertozzi, B., Brasseur, Z., Caudillo, L., Chen, D., Chu, B., Dada, L., Duplissy, J., Finkenzeller, H., Granzin, M., Guida, R., Heinritzi, M., Hofbauer, V., Iyer, S., Kempainen, D., Kong, W., Krechmer, J. E., Kürten, A., Lamkaddam, H., Lee, C. P., Lopez, B., Mahfouz, N. G. A., Manninen, H. E., Massabò, D., Mauldin, R. L., Mentler, B., Müller, T., Pfeifer, J., Philippov, M., Piedehierro, A. A., Roldin, P., Schobesberger, S., Simon, M., Stolzenburg, D., Tham, Y. J., Tomé, A., Umo, N. S., Wang, D., Wang, Y., Weber, S. K., Welti, A., Jonge, R. W. de, Wu, Y., Zauner-Wieczorek, M., Züst, F., Baltensperger, U., Curtius, J., Flagan, R. C., Hansel, A., Möhler, O., Petäjä, T., Volkamer, R., Kulmala, M., Lehtipalo, K., Rissanen, M., Kirkby, J., El-Haddad, I., Bianchi, F., Sipilä, M., Donahue, N. M., and Worsnop, D. R.: High Gas-Phase Methanesulfonic Acid Production in the OH-Initiated Oxidation of Dimethyl Sulfide at Low Temperatures, *Environ. Sci. Technol.*, 56, 13931–13944, <https://doi.org/10.1021/acs.est.2c05154>, 2022.

Steinke, M., Hodapp, B., Subhan, R., Bell, T. G., and Martin-Creuzburg, D.: Flux of the biogenic volatiles isoprene and dimethyl sulfide from an oligotrophic lake, *Sci. Rep.*, 8, 630, <https://doi.org/10.1038/s41598-017-18923-5>, 2018.

Tahan, A. and Shiroudi, A.: Oxidation reaction mechanism and kinetics between OH radicals and alkyl-substituted aliphatic thiols: H-abstraction pathways, *Prog. React. Kinet. Mech.*, 45, 1468678319886129, <https://doi.org/10.1177/1468678319886129>, 2020.

Wang, C., Xu, D., Bai, L., Zhu, B., Huang, L., and Jiang, H.: Effects of accumulated cyanobacterial bloom biomass contents on the characteristics of surface fluid sediments in a eutrophic shallow lake, *J. Environ. Manag.*, 308, 114644, <https://doi.org/10.1016/j.jenvman.2022.114644>, 2022.



- Wang, H., Zhang, Y., and Mu, Y.: Rate Constants for Reactions of •OH with Several Reduced Sulfur Compounds Determined by Relative Rate Constant Method, *Acta Phys.-Chim. Sin.*, 24, 945–950, [https://doi.org/10.1016/s1872-1508\(08\)60041-8](https://doi.org/10.1016/s1872-1508(08)60041-8), 2008.
- Wang, J., Xu, G., Chen, L., and Chen, K.: Atmospheric Particle Number Concentrations and New Particle Formation over the Southern Ocean and Antarctica: A Critical Review, *Atmosphere*, 14, 402, <https://doi.org/10.3390/atmos14020402>, 2023a.
- Wang, J., Chu, Y.-X., Tian, G., and He, R.: Estimation of sulfur fate and contribution to VSC emissions from lakes during algae decay, *Sci. Total Environ.*, 856, 159193, <https://doi.org/10.1016/j.scitotenv.2022.159193>, 2023b.
- Wang, J., Wei, Z.-P., Chu, Y.-X., Tian, G., and He, R.: Eutrophication levels increase sulfur biotransformation and emissions from sediments of Lake Taihu, *Sci. Total Environ.*, 887, 164054, <https://doi.org/10.1016/j.scitotenv.2023.164054>, 2023c.
- Wang, K., Ge, M., and Wang, W.: Temperature dependent kinetics of the gas-phase reaction of OH radicals with EMS, *Chin. Sci. Bull.*, 56, 391–396, <https://doi.org/10.1007/s11434-010-4313-y>, 2011.
- Wang, M., Xu, X., Wu, Z., Zhang, X., Sun, P., Wen, Y., Wang, Z., Lu, X., Zhang, W., Wang, X., and Tong, Y.: Seasonal Pattern of Nutrient Limitation in a Eutrophic Lake and Quantitative Analysis of the Impacts from Internal Nutrient Cycling, *Environ. Sci. Technol.*, 53, 13675–13686, <https://doi.org/10.1021/acs.est.9b04266>, 2019.
- Wang, Y., Mehra, A., Krechmer, J. E., Yang, G., Hu, X., Lu, Y., Lambe, A., Canagaratna, M., Chen, J., Worsnop, D., Coe, H., and Wang, L.: Oxygenated products formed from OH-initiated reactions of trimethylbenzene: Autoxidation and accretion, *Atmos. Chem. Phys. Discuss.*, 2020, 1–32, <https://doi.org/10.5194/acp-2020-165>, 2020.
- Wine, P. H., Kreutter, N. M., Gump, C. A., and Ravishankara, A. R.: Kinetics of hydroxyl radical reactions with the atmospheric sulfur compounds hydrogen sulfide, methanethiol, ethanethiol, and dimethyl disulfide, *J. Phys. Chem.*, 85, 2660–2665, <https://doi.org/10.1021/j150618a019>, 1981.
- Wine, P. H., Thompson, R. J., and Semmes, D. H.: Kinetics of OH reactions with aliphatic thiols, *Int. J. Chem. Kinet.*, 16, 1623–1636, <https://doi.org/10.1002/kin.550161215>, 1984.
- Xu, H., McCarthy, M. J., Paerl, H. W., Brookes, J. D., Zhu, G., Hall, N. S., Qin, B., Zhang, Y., Zhu, M., Hampel, J. J., Newell, S. E., and Gardner, W. S.: Contributions of external nutrient loading and internal cycling to cyanobacterial bloom dynamics in Lake Taihu, China: Implications for nutrient management, *Limnol. Oceanogr.*, 66, 1492–1509, <https://doi.org/10.1002/lno.11700>, 2021.
- Ye, Q., Goss, M. B., Krechmer, J. E., Majluf, F., Zaytsev, A., Li, Y., Roscioli, J. R., Canagaratna, M., Keutsch, F. N., Heald, C. L., and Kroll, J. H.: Product distribution, kinetics, and aerosol formation from the OH oxidation of dimethyl sulfide under different RO₂ regimes, *Atmos. Chem. Phys.*, 22, 16003–16015, <https://doi.org/10.5194/acp-22-16003-2022>, 2022.



Yu, C., Shi, C., Ji, M., Xu, X., Zhang, Z., Ma, J., and Wang, G.: Taste and odor compounds associated with aquatic plants in Taihu Lake: distribution and producing potential, *Environ. Sci. Pollut. Res.*, 26, 34510–34520, <https://doi.org/10.1007/s11356-019-06188-6>, 2019a.

Yu, Y., Li, C., Shen, W., Wang, Z., Xu, P., and Yu, H.: Volatile compounds released by microalgae-water phase from Taihu Lake in China, *Harmful Algae*, 84, 56–63, <https://doi.org/10.1016/j.hal.2019.01.009>, 2019b.

Zhao, Y., Schlundt, C., Booge, D., and Bange, H. W.: A decade of dimethyl sulfide (DMS), dimethylsulfoniopropionate (DMSP) and dimethyl sulfoxide (DMSO) measurements in the southwestern Baltic Sea, *Biogeosciences*, 18, 2161–2179, <https://doi.org/10.5194/bg-18-2161-2021>, 2021.

Zhou, C., Xu, X., Peng, Y., Wang, G., Liu, H., Jin, Q., Jia, R., Ma, J., Kinouchi, T., and Wang, G.: Response of sulfate concentration to eutrophication on spatio-temporal scale in freshwater lakes, *Sci. Total Environ.*, 953, 176142, <https://doi.org/10.1016/j.scitotenv.2024.176142>, 2024.